Journal of Marine Research, 65, 169–192, 2007

Hurricane-induced destratification and restratification in a partially-mixed estuary

by Ming Li[1,2], Liejun Zhong[1], William C. Boicourt[1], Shunli Zhang[3] and Da-Lin Zhang[3]

ABSTRACT

Hurricane Isabel made landfall at the Outer Banks of North Carolina and moved past Chesapeake Bay on 18–19 September 2003. The baroclinic response of this partially-mixed estuary to the passage of Isabel is investigated using the output from a regional atmosphere-ocean model. The hurricane-forced winds caused gradual deepening of the surface mixed layer, followed by rapid destratification in the water-column. The mixed-layer deepening appears to be driven by velocity shear and can be interpreted by a gradient Richardson number. Although strong winds caused complete mixing locally, a large longitudinal salinity gradient of about 10^{-4} psu m^{-1} persisted between the estuary's head and mouth. After passage of the storm, the horizontal baroclinic pressure gradient drove restratification and a two-layer circulation in the estuary. The averaged buoyancy frequency increased linearly with time during an initial stage, and reached about 0.03 s^{-1} one day after the destratification. The model results are in good agreement with the theoretical prediction based on gravitational adjustment. Subsequently, turbulent diffusion works against the longitudinal advection to produce quasi-steady salinity distribution.

1. Introduction

Chesapeake Bay is a partially-mixed estuary featuring a two-layer residual circulation. The water column is stratified with the vertical salinity difference ranging between 2 and 10 (Carter and Pritchard, 1988). The strength of vertical stratification in the Bay is primarily controlled by the amount of river runoff. Anthropogenic nutrient enrichment has led to excessive algal production and the associated depletion of oxygen from bottom water in the Bay (Kemp *et al.*, 2005). Physical processes play a crucial role in the establishment, maintenance and termination of hypoxia (Boicourt, 1992). In particular, strong winds can destratify the water column and re-aerate the bottom water (Goodrich *et al.*, 1987). After the winds subside, the longitudinal salinity gradient between the estuary's mouth and head may cause restratification, sometimes resulting in a quick return of hypoxia. Therefore, it is important to understand the physics of storm-induced destratification and restratification in

1. Horn Point Laboratory, University of Maryland Center for Environmental Science, P. O. Box 775, Cambridge, Maryland, 21613, U.S.A.

2. Corresponding author. ***email: mingli@hpl.umces.edu***

3. Department of Atmospheric and Oceanic Science, University of Maryland, College Park, Maryland, 20742, U. S. A.

an estuary and examine how hurricanes and other storms contribute to the termination of hypoxia in the fall.

On 18 September 2003, Category 2 Hurricane Isabel made landfall over the Outer Banks of North Carolina and moved northward on the west side of Chesapeake Bay. The mid-Bay buoy of the Chesapeake Bay Observing System (CBOS) survived the passage of Isabel and provided real-time current measurements (see http://www.cbos.org). Strong northwestward winds forced water in Chesapeake Bay to move northward, producing high sea levels and flooding in Washington, D.C., Baltimore and Annapolis (Boicourt, 2005). Post-Isabel field surveys showed that the storm led to enhanced plankton and fish abundance in Chesapeake Bay (Roman *et al.*, 2005). Ocean color measurements from aircraft revealed an unusually strong fall bloom of phytoplankton over the middle and lower Bay. Miller *et al.* (2006) speculated that wind mixing de-stratified the water columns and injected nitrogen into the euphotic layer while the subsequent re-stratification maintained phytoplankton in well-illuminated surface water. However, restratification probably diminished vertical mixing and allowed biological consumption to draw down oxygen concentration, resulting in a quick return of hypoxia in the Bay (Boicourt, 2005).

We have conducted numerical simulations of Hurricane Isabel using a coupled regional atmosphere-ocean model. The regional atmosphere model is based on the fifth-generation Penn State University/National Center for Atmospheric Research model (MM5) and has a horizontal resolution of 4 km over the Chesapeake Bay region (see http://www.atmos.umd.edu/~mm5; *Grell et al.*, 1995). The model provided accurate predictions for the trajectory and intensity of Hurricane Isabel (2003) as well as all the meteorological fields including wind stress over the Bay. The regional ocean model of Chesapeake Bay is based on the Regional Ocean Modeling System (ROMS) (Li *et al.*, 2005b). It has a horizontal resolution of about 1 km and 20 vertical layers. It accurately predicted the storm surges and wind-driven currents generated by Isabel. Detailed results on the storm surge prediction can be found in Li *et al.* (2006). In this paper we investigate the baroclinic response of Chesapeake Bay to the passage of Isabel.

Wind-induced destratification was previously observed in Chesapeake Bay but wind speeds were much lower than those recorded during the passage of Hurricane Isabel. Goodrich *et al.* (1987) reported that destratification occurs between early fall and middle spring. They calculated gradient Richardson numbers (*Ri*) using surface and bottom velocities and salinities at a continuous monitoring station, and found that low *Ri* values preceded destratification events. Subsequently, Blumberg and Goodrich (1990) used the Princeton Ocean Model to simulate wind-induced destratification over a 4-week period in 1983, but they did not examine the restratification process. Due to constraints in computing power at that time, the model used coarse grid resolution (10 –15 km in horizontal directions and 10 vertical levels). Both the data analysis and modeling study focused on time series at fixed locations and did not provide a complete picture of mixing and destratification over the whole Bay. An outstanding question was whether the destratification extends everywhere or is limited to certain geographic regions. Thus, the first goal of

this paper is to obtain further insights into the physics of storm-driven turbulent mixing in a partially-mixed estuary.

The second goal of this paper is to explore the physics of post-storm restratification process. Simpson and Linden (1989) studied gravitational adjustment of a fluid containing a horizontal density gradient. For the case of uniform density gradient, they found an analytic solution in which buoyancy frequency increases linearly with time and *Ri* is ½. If the horizontal density gradient is nonuniform, frontogenesis was predicted to occur on the isopycnal between the constant-density-gradient regions. Simpson and Linden (1989) conducted laboratory experiments which confirmed the theoretical predictions. When rotational effect is important, however, the fluid undergoes geostrophic adjustment rather than gravitational adjustment. Tandon and Garrett (1994, 1995) showed that buoyancy frequency scales with the horizontal buoyancy gradient over the Coriolis parameter and that the geostrophically-adjusted steady-state *Ri* is 1. In the absence of damping, a constant horizontal density gradient may lead to inertial oscillations of isopycnals with $Ri = ½$ (Tandon and Garrett, 1994). These theoretical calculations assume that no external force is generating turbulent mixing during the adjustment phase while *Ri* values of ½ or 1 suggest no instability arising from the adjustment itself. A new study by Boccaletti *et al.* (2007), however, shows that secondary instabilities can arise along the adjusting fronts, following the initial restratification phase described by Tandon and Garrett (1994, 1995). Agoestrophic baroclinic instabilities may develop along these fronts and cause the horizontal density gradients to slump under the influence of rotation.

In the open ocean, mixed-layer restratification has been observed following wind storms or night-time convection. Brainerd and Gregg (1993a, b) observed that lateral interleaving driven by horizontal density gradient significantly increases the growth of vertical buoyancy gradient in restratifying mixed layers beyond that resulting from insolation and vertical turbulent fluxes. Rudnick and Ferrari (1999) found that the mixed layers along 1000-km tows in the northeast Pacific were filled by temperature-salinity structures that were density compensating at scales smaller than 10 km. They hypothesized that these structures resulted from the slumping of lateral density contrasts within the mixed layers. Young (1994) developed a subinertial mixed-layer theory to incorporate this effect into three-dimensional mixed-layer models. In contrast, there have been few investigations into the restratification process in coastal and estuarine waters.

The paper is organized as follows. Section 2 describes the model configuration. Section 3 examines storm-induced mixing and destratification, and Section 4 shows the horizontally-driven restratification. Concluding remarks are given in section 5.

2. Regional atmosphere-ocean models

To simulate the response of Chesapeake Bay to Hurricane Isabel, we have coupled a three-dimensional hydrodynamic model of Chesapeake Bay with a regional atmospheric model for the Middle Atlantic Region. The atmospheric model was used in real-time

forecasting mode to provide hurricane predictions while the oceanic model was run in hindcast mode.

A nested-grid (4/12/36 km) version of the MM5 has been used since 1998 to provide real-time forecasts for the Mid-Atlantic Region (MAR) at the University of Maryland (see http://www.atmos.umd.edu/~mm5 for model details). The vertical discretization uses terrain-following σ-coordinates, but pressure at the σ-levels is determined from a reference state that is estimated using the hydrostatic equation from a given sea-level pressure and temperature with a standard lapse rate. There are 30 uneven σ levels, giving 29 layers, with higher resolution in the planetary boundary layer (PBL). The surface layer is defined at an altitude of about 10 m, the level at which surface winds are typically observed. The model top is set at 50 hPa with a radiative top boundary condition. The important model physics of MM5 relevant to the hurricane prediction includes: (i) the latest version of the Kain-Fritsch convective scheme (Kain and Fritsch, 1993); (ii) an explicit moisture scheme (without the mixed phase) containing prognostic equations for cloud water (ice) and rainwater (snow) (Dudhia, 1989; Zhang, 1989); (iii) a modified version of the Blackadar (PBL) scheme (Zhang and Anthes, 1982); (iv) a simple radiative cooling scheme (Grell *et al.*, 1995); and (v) a multi-layer soil model to predict land surface temperatures using the surface energy budget equation (Dudhia, 1989).

MM5 provided reasonable predictions for the trajectory and intensity of Hurricane Isabel as well as all the meteorological fields, including the wind stress field over Chesapeake Bay at the horizontal resolution of 4 km. Figure 1 shows the predicted and observed hurricane tracks as well as a snapshot of the surface wind stress field at 0000 LST 19 September 2003. The predicted track is in close proximity to the observed until 0600 LST 19 September when the storm's influence on the Bay starts to diminish. A comparison between the predicted and observed wind speeds can be found in Li *et al.* (2006).

Regional Ocean Modeling System (ROMS) is the state-of-art regional ocean model based on primitive equations (Shchepetkin and McWilliams, 2005). Li *et al.* (2005b) configured it for Chesapeake Bay and its tributaries. The Bay is shallow in most places, but a deep paleochannel running in the north-south direction dominates the bathymetry in the middle reaches of the main Bay (Fig. 2a). An orthogonal curvilinear coordinate system is designed to follow the center channel and coastlines of the main stem (Fig. 2b). The grid spacing is less than 1 km in the cross-channel direction and about 2-3 km in the along-channel direction. The total number of grid points is 120×80. The model has 20 layers in the vertical direction. A quadratic stress is exerted at the bed, assuming that the bottom boundary layer is logarithmic over a roughness height of 0.5 mm. The vertical eddy viscosity and diffusivity are computed using the modified Mellor-Yamada (*k-kl*) turbulence closure scheme incorporated into ROMS (Warner *et al.*, 2005). Li *et al.* (2005b) examined the sensitivity of model predictions to four turbulence closure schemes (*k-kl*, *k-*ϵ, *k-*ω and KPP models) but found little differences in the model results. By validating against three-dimensional (along-channel and cross-channel) hydrographic surveys and salinity time series collected at the surface and bottom depths, Li *et al.* (2005b) found that the *k-kl*

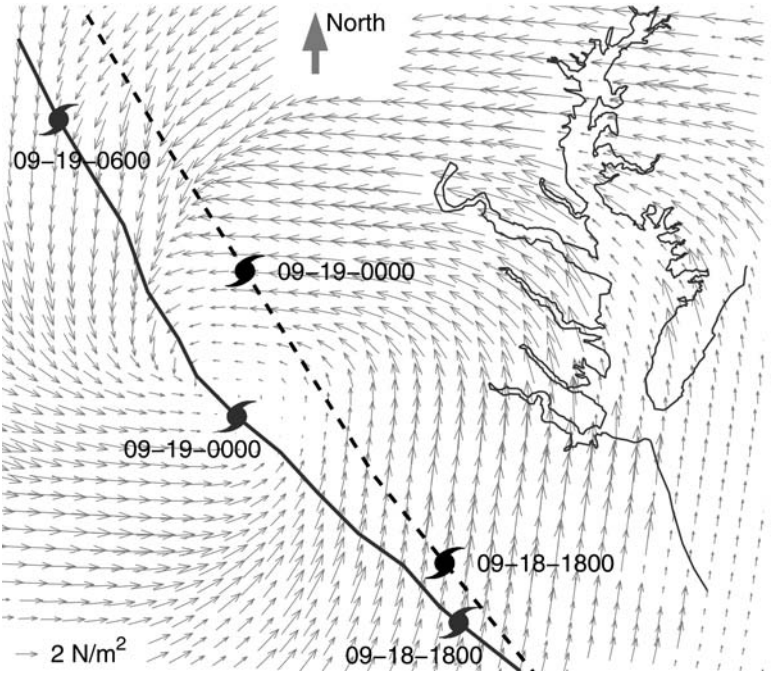

Figure 1. The MM5-predicted surface wind stress field at 0000 LST 19 September 2003, with the predicted (solid) and observed (dashed) tracks of Hurricane Isabel.

scheme with a background diffusivity of 10^{-5} m^2 s^{-1} provides the best match with the observational data. The averaged skill for the salinity prediction is 0.82. (A score of 1.0 means a perfect agreement between the data and model predictions.) This turbulence parameterization scheme was employed in this study, but other formulations were also examined to ensure that the results were not sensitive to the choice of closure. Coefficients of horizontal eddy viscosity and diffusivity are set to 1 m^2 s^{-1}, which should produce little dissipation of the resolved flow energy (c.-f. Zhong and Li, 2006).

The ROMS model is forced by sea level at the open ocean boundary, by freshwater inflows at river heads, and by wind and heat exchange across the water surface. Tidal elevation at the open boundary is decomposed into five major tidal constituents, M_2, S_2, N_2, K_1, O_1, using the harmonic constants linearly interpolated from the Oregon State University (OSU) global inverse tidal model TPXO.6.2 (Egbert and Erofeeva, 2002). Nontidal coastal sea-level fluctuations are specified using detided sea-level records at two tidal stations: Duck, North Carolina, and Kiptopeake, Virginia (see Fig. 2b for their locations). The latter is used because Wachapreague station outside the Bay's mouth was out of order during the passage of Isabel. The open-ocean boundary condition for the barotropic component consists of Chapman's condition for surface elevation and Flather's condition for barotropic velocity. The boundary condition for the baroclinic component includes an

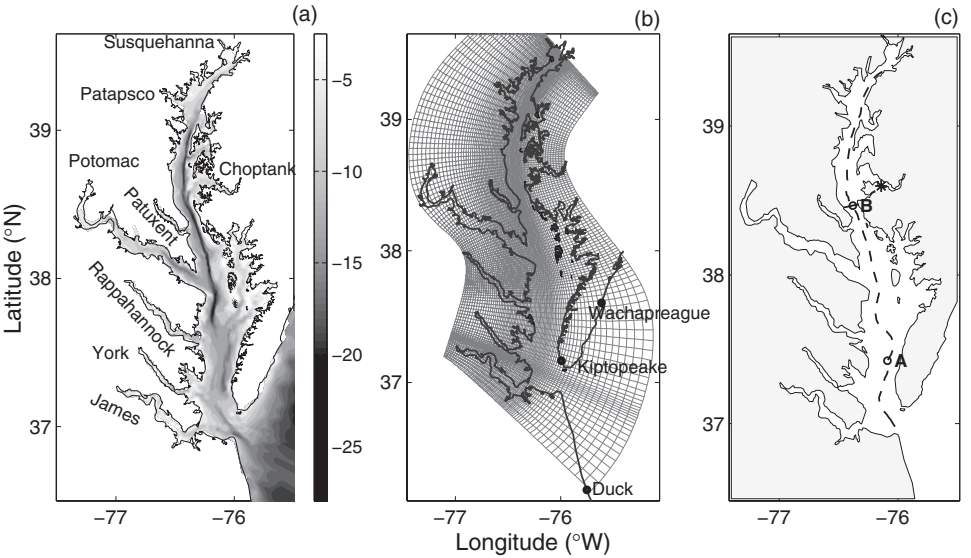

Figure 2. (a) Bathymetry of Chesapeake Bay and its adjacent coastal area. Depth scales are in metres. (b) the horizontal curvilinear coordinate system, and (c) along-channel (dashed) and cross-channel (solid) sections used in the present analysis. The open circle marked by "A" denotes a lower-Bay station while "B" denotes the mid-Bay station of the Chesapeake Bay Observing System (CBOS). The symbol "*" marks a mid-Bay weather station.

Orlanski-type radiation condition for baroclinic velocity. To deal with both inward and outward scalar fluxes across the open boundary, we use a combination of radiation condition and nudging (with a relaxation time scale of 1 day) for temperature and salinity, following the recommendation by Marchesiello *et al.* (2001). Salinity and temperature fields on the offshore open boundary are prescribed using the monthly Levitus climatology combined with the field data at Duck, North Carolina, acquired by the Field Research Facility of the U.S. Army Corps of Engineers.

Chesapeake Bay has eight major tributaries: the Susquehanna, Patapsco, Patuxent, Potomac, Rappahannock, York, James and Choptank Rivers. The Susquehanna River, the Potomac River and the James River are the three largest tributaries in terms of fresh- water input. Figure 3a shows time series of their discharge over a two-month period covering Hurricane Isabel. At the upstream boundary in the eight major tributaries, the daily freshwater inflow is prescribed with zero salinity and time-varying temperature. Hourly wind stress fields produced by the MM5 atmospheric model are used to drive the ROMS model for Chesapeake Bay. Figure 3b shows the time series of predicted wind speed at a weather station close to the CBOS mid-Bay buoy (see its location in Fig. 2c). The wind switched from southward to northward directions as Hurricane Isabel moved past Chesapeake Bay.

The ROMS model was run for the period between 1 August and 30 September, 2003.

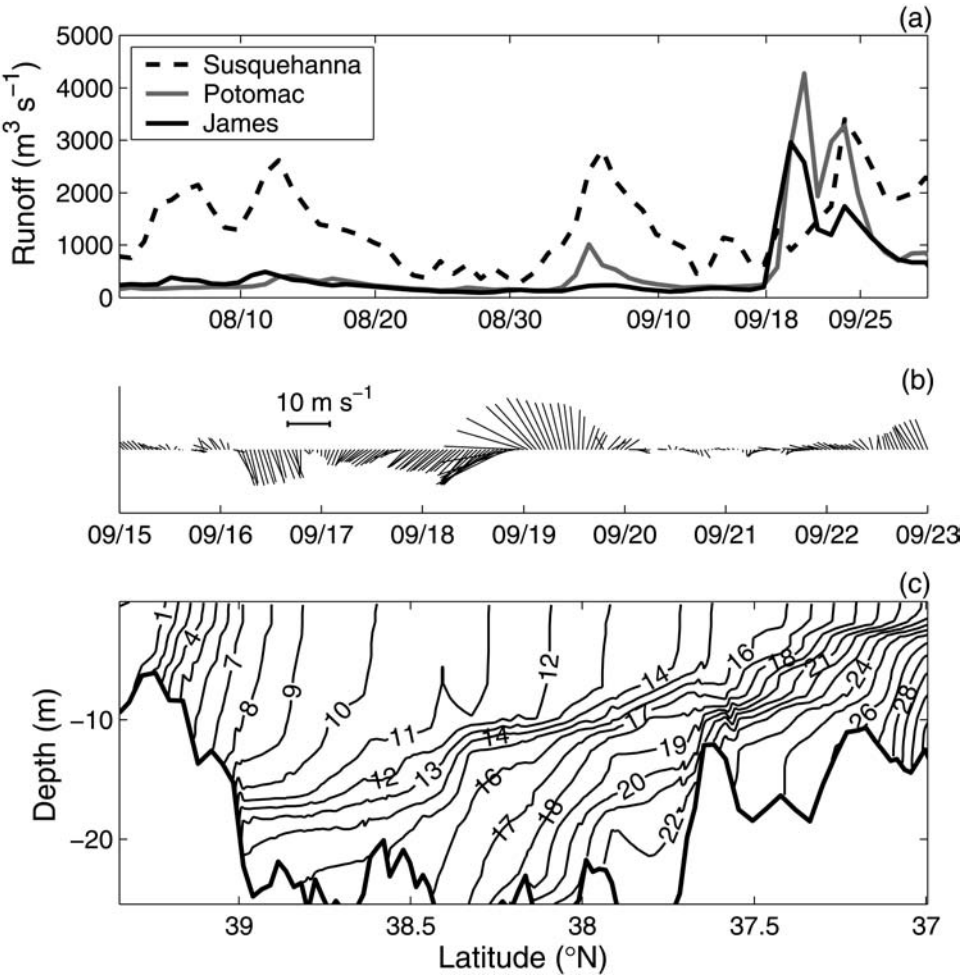

Figure 3. (a) Observed stream flows from the Susquehanna (dashed), Potomac (grey) and James (solid) rivers, (b) time series of the predicted wind speed vectors at the mid-Bay weather station and (c) the initial salinity distribution in the along-channel section.

The initial temperature and salinity fields were constructed from the sampling data collected by the Environmental Protection Agency Chesapeake Bay Program (see Fig. 3c for the initial salinity field in the along-channel section). The initial velocity field was taken to be zero, and the water surface was set at the mean sea level. Since the Isabel's eye passed Chesapeake Bay on the landward side, we did not consider the small inverse barometer effect. Neither were the effects of surface waves considered. We may anticipate more accurate predictions if these effects were incorporated; they will be worthwhile to pursue in the future.

3. Storm-induced mixing and destratification

Winds generate turbulent mixing in the ocean either through wind stress or through vertical shear in the wind-driven currents. The wind stress produces a turbulent boundary layer which mixes surface water directly. In a semi-enclosed water body such as Chesapeake Bay, the surface water may be frictionally coupled to the wind whereas the bottom water responds to the wind-generated slope and is driven in the opposite direction (Wang, 1979a; Vieira, 1986). This differential response of surface and bottom water to wind forcing may produce large internal velocity shear and strong turbulent mixing at mid-depths (Blumberg and Goodrich, 1990). Based on results from a coarse-resolution numerical model, Blumberg and Goodrich (1990) suggested that internal shear provides a more effective mechanism for mixing than direct propagation of turbulence from the surface. In this section we will examine the mixing and destratification caused by Hurricane Isabel and ascertain mechanisms of turbulent mixing.

As a first step, we examine the time series of the model-predicted currents and stratification at a mid-Bay station. The Chesapeake Bay Observing System (CBOS) mid-Bay buoy provided real-time current observations during the passage of Hurricane Isabel (see http://www.cbos.org) that are compared to the predicted currents in Figure 5. The buoy is located in the deep channel of the Bay, approximately 100 km seaward of the Susquehanna River mouth (see Fig. 2c for its location). In Figure 4a we plot the predicted time series of top-bottom salinity difference at this buoy station. This difference was 4 prior to the storm, decreasing to zero during the storm, but recovering to about 2 after the storm. Unfortunately, salinity sensors attached to the CBOS buoy were contaminated by biofouling so that salinity data could not be used to validate the model prediction. To inquire if internal shear or surface wind stress was likely responsible for the destratification, we calculate two dimensionless parameters using model outputs: Ri based on the velocity and salinity at the surface and bottom; bulk Richardson number $Rb = B/\bar{u}^2$ where $\bar{u}$ is the averaged velocity for the mixed layer, and

$$B = \frac{g}{p}\int_{-h}^{0} [p(-h,t) - p(z,t)]dz$$

the vertically-integrated buoyancy anomaly (h is the surface mixed-layer depth; e.g., Trowbridge, 1992). If surface stress causes the mixed-layer deepening, Rb is expected to fall below a threshold. If internal shear causes the turbulent mixing, Ri is expected to fall below ¼. As shown in Figure 4b, Ri falls below ¼ during the passage of Isabel and stays above it at other times. In contrast, Rb shows wild fluctuations that are difficult to interpret (Fig. 4c, a definition of the mixed-layer depth will be given later when results in Fig. 5 are discussed). It appears that the gradient Richardson number based on the surface-bottom velocity and density differences is a better indicator of the destratification process at the CBOS mid-Bay site.

On the CBOS mid-Bay buoy, three fixed-depth conventional current meters were

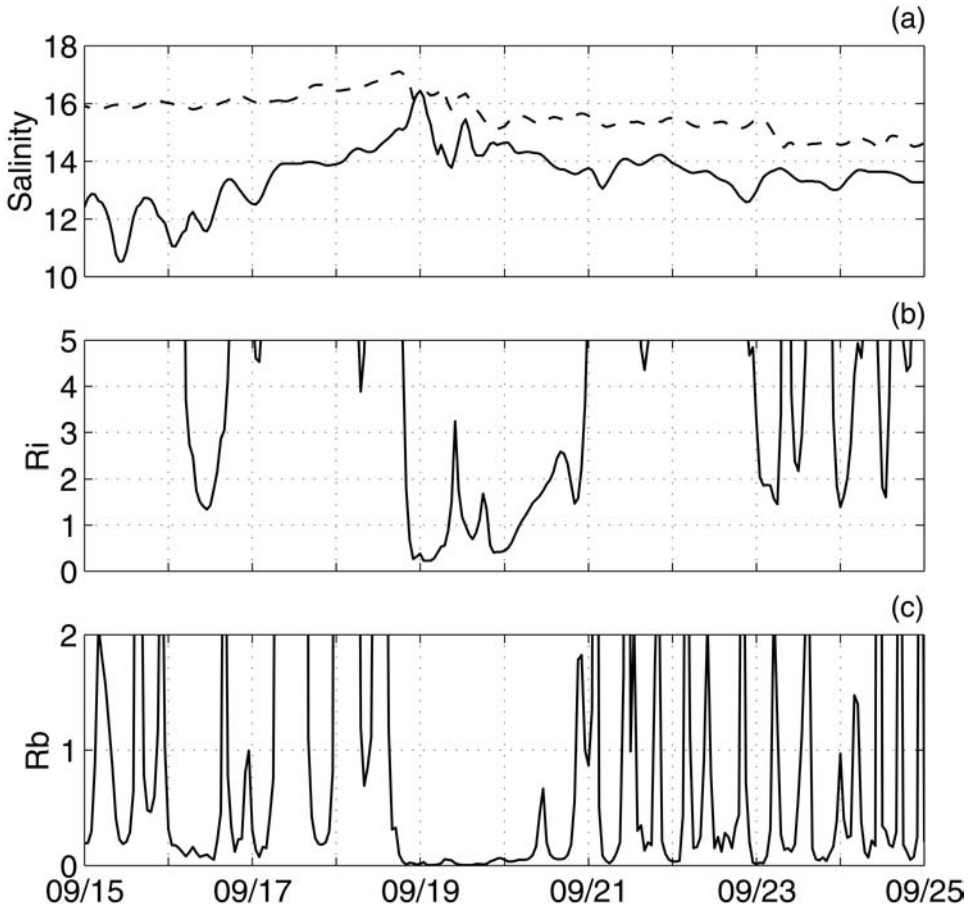

Figure 4. Time series of (a) surface (solid) and bottom (dashed) salinity, (b) gradient Richardson number calculated from the surface and bottom velocities and salinities, and (c) bulk Richardson number calculated using the mean velocity and buoyancy in the surface mixed layer at CBOS mid-Bay buoy site.

deployed to obtain flow measurements at 2.4, 10 and 19 m depths, but the current-meter at 19 m was out of order at the time. Figures 5b-d show the predicted and observed current speeds at the site. Before 16 September, winds were weak (Figs. 3b and 5a) and a classical two-layer current structure was superposed on the regular ebb-and-flood of the semidiurnal tide. Accordingly, the bed stress exhibited periodic fluctuations with larger (positive) values occurring during flood tides (Fig. 5a). As Isabel moved towards the Outer Banks of North Carolina between 16 and 18 September, southward winds blew over Chesapeake Bay and its adjacent shelf (see Fig. 3b). According to Blumberg and Goodrich (1990), this southward wind would drive two-layer flows which amplify the gravitational circulation. The velocity at 2.4 m was expected to remain positive and increase in magnitude.

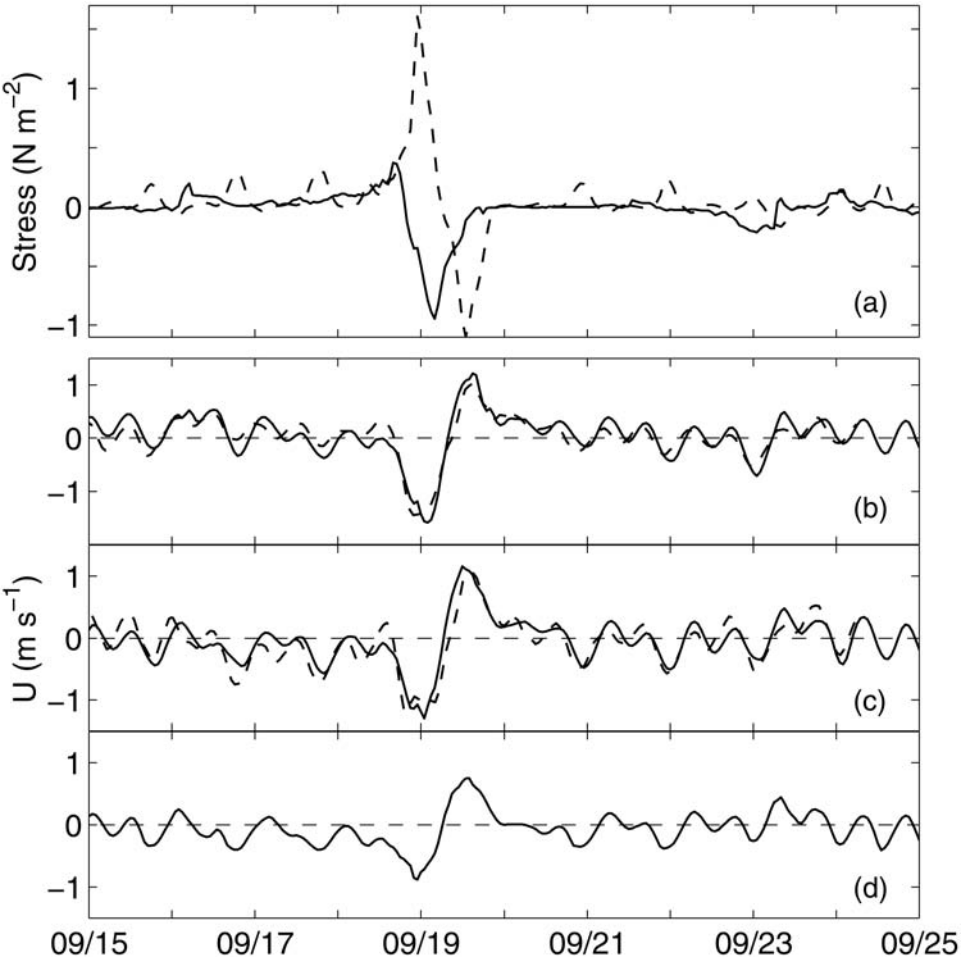

Figure 5. Time series of the north-south component of (a) wind stress (solid) and bed stress (dashed), predicted (solid) and observed (dashed) currents at (b) 2.4-m, (c) 10-m and (d) 19-m depths at CBOS Mid-Bay buoy site. Positive values correspond to southward winds and seaward currents.

Surprisingly, this anticipated response was not observed (Fig. 5b). Instead currents at all three depths shifted in the landward (negative) direction. After Isabel made landfall in the evening of 18 September, the storm's northwest-to-northward winds became so strong to force the entire water column up the Bay at speeds in excess of 1.0 m s^{-1}. After the storm's passage, the Bay relaxed with a rapid movement of the entire water column in an opposite direction. The observed current variability was well captured by the model. The root-mean-square error between the predicted and observed currents is about 0.19 m s^{-1} and the model has a high predictive skill of 0.93 (see Li *et al.*, 2006).

The surprising response observed prior to Isabel's landfall hints that factors other than

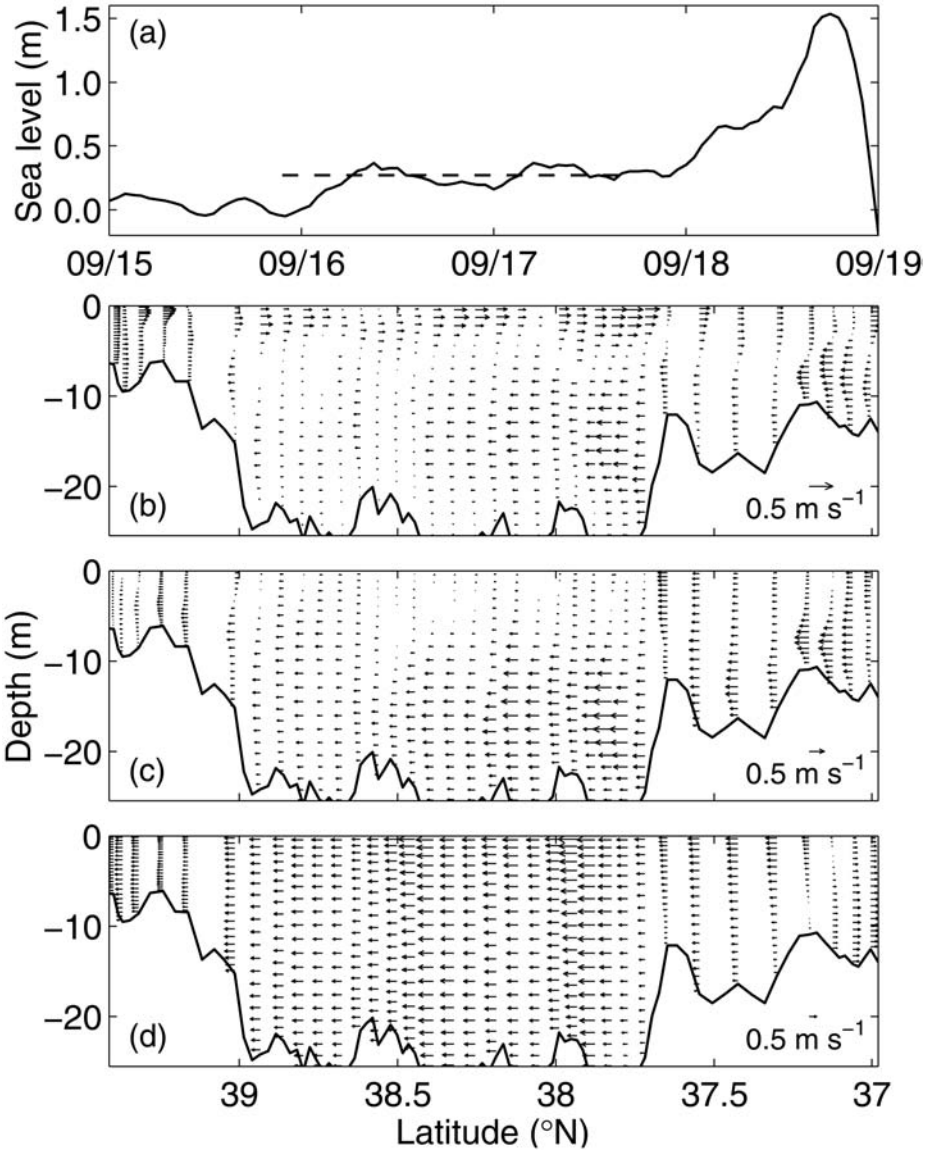

Figure 6. (a) Time series of mouth-head sea level difference in the estuary. The dashed line indicates the average height difference prior to Isabel's landfall. Nontidal longitudinal velocity distribution in the along-channel section at (b) 0000 LST 16, (c) 1200 LST 17 and (d) 0000 LST 19 September 2003.

the local wind stress might be responsible for generating the currents in the Bay. In Figure 6a, we plot the sea-level difference between the Bay's mouth and head. We use the harmonic method given in Zhong and Li (2006) to remove tidal components. We also

subtract the sea level slope associated with the fresh-water discharge at the estuary head. This sea level slope is balanced by the baroclinic pressure gradient associated with sloping isopycnals and is not part of the wind-driven circulation. As shown in Figure 6a, sea level at the mouth is about 0.3 m higher between 16 and 18 September. Two different factors contribute to this sea-level difference. First, the southward winds blowing over the Bay surface drive water seaward and cause sea-level to drop near its head. If this sea level slope balances the lateral average of wind stress divided by water depth, then there tends to be flow in the direction of the wind in shallow shoals, but in the opposite direction in the deep channel, as shown by Csanady (1973) for a lake. Secondly, the southward winds blowing over the shelf drive an onshore Ekman flux and cause sea level to rise at the Bay's mouth (e.g., Wang, 1979b; Garvine, 1985). The sloping sea surface produces a landward-directed pressure gradient which opposes the local wind stress. We can compare the magnitude of these two terms in the momentum equation. The depth-integrated pressure force is $\rho g H \partial \eta / \partial x$ where ρ is the water density, g the gravitational constant, H the averaged water depth and $\partial \eta / \partial x$ is the sea-level slope. Using $H = 10$ m and $\partial \eta / \partial x \approx 0.3$ m/300 km, we obtain $\rho g H \partial \eta / \partial x \approx 0.1$ Nm^{-2}. On the other hand, the southward (positive) wind stress averaged to about 0.1 Nm^{-2} before landfall (see Fig. 5a). Therefore, both the landward sea-level slope and local wind stress appear to be equally important in driving the currents in the Bay prior to Isabel's landfall. This result on the local and remote wind forcing of Chesapeake Bay is in general agreement with the findings in Delaware Bay (Wong and Garvine, 1984; Janzen and Wong, 2002). In particular, Janzen and Wong (2002) showed that the remote wind affects sea level and vertically-averaged flow while the local winds drive a two-layer circulation, with the surface layer moving downwind and the bottom layer moving upwind.

Snapshots of nontidal velocity distribution in the along-channel section are shown in Figures 6b-d. Tidal velocity components are removed using the harmonic analysis method (Zhong and Li, 2006). At 0000 LST 16 September, the velocity field shows the classic two-layer estuarine circulation: seaward flow in the surface layer and landward flow in the bottom layer (Fig. 6b). By 1200 LST 17 September, however, the circulation pattern became very different. Water at all depths in the lower Bay moved toward the head, while current velocity in the surface layer of the mid-Bay dropped to small values (Fig. 6c). The sloping sea surface overcame the southward winds in driving landward flow in the shallow lower Bay and offset the local wind stress in the surface layer of the deeper mid-Bay. The landward flow strengthened and penetrated further upstream as Isabel approached the coast. At the peak of the storm (i.e., 0000 LST 19 September), the northward winds and incoming storm surge drove strong landward currents everywhere in the estuary (Fig. 6d), resulting in high sea levels in the upper Bay. This setup at the estuary head produced a seaward pressure gradient, which subsequently drove strong seaward flows after the passage of the storm (see Figs. 5b-d).

To examine how the hurricane-forced winds and currents change density structure in the water column, we plot the time-depth distribution of salinity at the CBOS mid-Bay site as

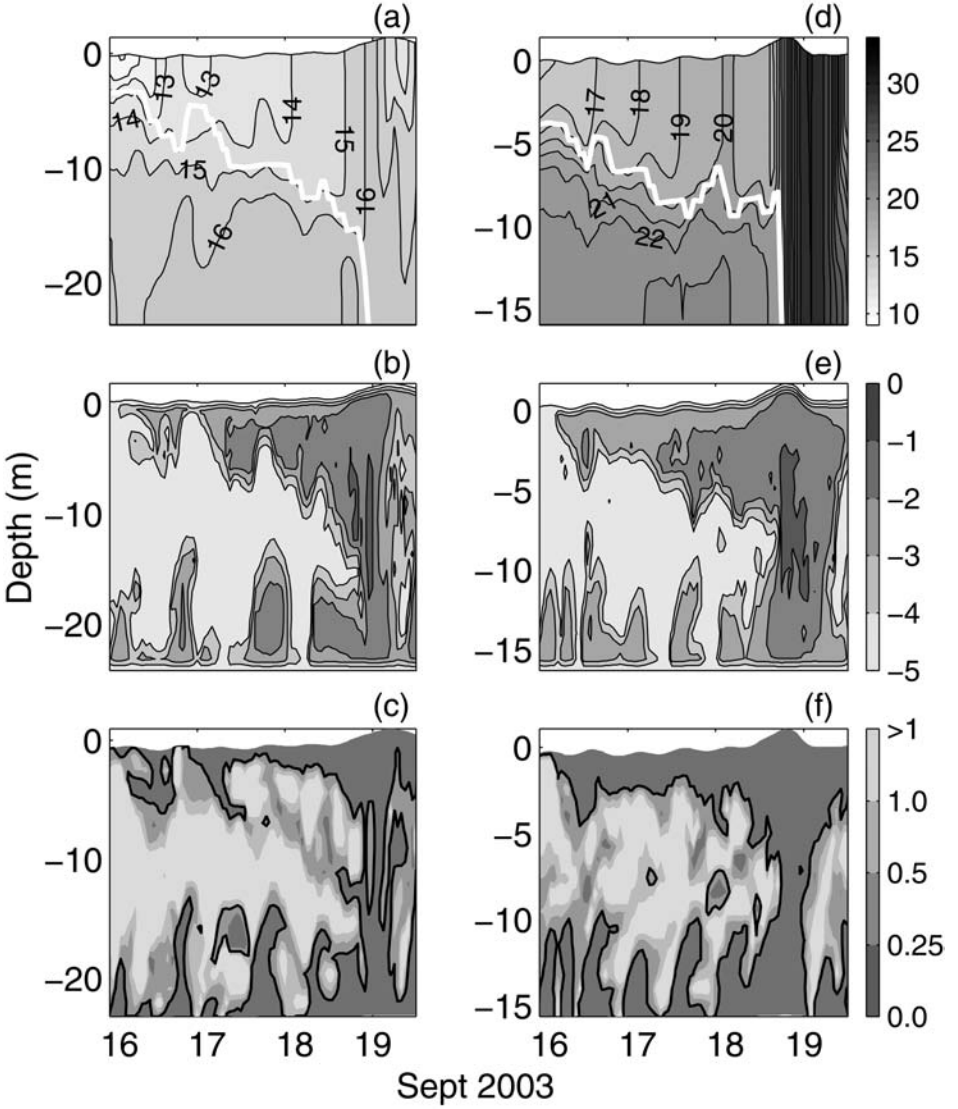

Figure 7. Time evolution of (a, d) salinity, (b, e) logarithm of vertical diffusivity ($m^2 s^{-1}$) and (c, f) gradient Richardson number at the mid Bay (left panel) and lower Bay (right panel) stations. White lines in (a, d) show the estimated mixed-layer depth.

well as at a shallower lower-Bay site in Figure 7 (see Fig. 2c for its location). To aid discussion, we also plot the depth of the surface mixed layer. The mixed-layer depth is defined to be the depth where the vertical salinity gradient (i.e., buoyancy frequency) reaches a maximum. This criterion was used by Li and Garrett (1995) to investigate the deepening of the ocean mixed layer driven by Langmuir circulation. At the mid-Bay

station, the mixed layer deepened gradually from 4 m on 16 September to 15 m on 18 September (Fig. 7a). Shortly after Isabel's landfall, stratification in the water column was completely destroyed, as shown by the vertical isohalines.

Although there were no turbulence measurements in the Bay during the passage of Hurricane Isabel, we can diagnose vertical eddy diffusivity Kv from the model and examine its temporal evolution (Fig. 7b). Strong mixing was concentrated in the surface and bottom boundary layers before landfall. Kv increased from 10^{-4} to 10^{-2} m^2 s^{-1} in the surface mixed layer while Kv reached 10^{-2} m^2 s^{-1} in the bottom boundary layer and showed a periodic fluctuation at the M_4 tidal frequency. In contrast, turbulent mixing was weak in the interior pycnocline region before landfall. At the time of complete destratification, the surface and bottom boundary layers appear to have merged and the highest eddy diffusivity of 0.1 - 1 m^2 s^{-1} is found at mid-depths. We diagnosed *Ri* from the local velocity and density gradients (Fig. 7c). Low *Ri* ($<$¼) regions were confined to the surface and bottom boundary layers and generally correlated with high diffusivity regions. Prior to Isabel's arrival, *Ri* exceeded ¼ in the pycnocline region but low Ri values expanded to the whole column after destratification. The good correspondence between Kv and *Ri* distributions suggests that the local shear was likely responsible for generating turbulent mixing. Unlike the previous findings of Goodrich *et al*. (1987) and Blumberg and Goodrich (1990), the pre-landfall southward winds did not generate large internal shear and strong interior mixing. Instead, turbulent mixing was initiated in the boundary layers and subsequently filled in the whole water column. This result is not inconsistent with Figure 4c which shows that the bulk Richardson number *Rb* fails to provide a good prediction for the mixed-layer deepening. The one-dimensional mixed-layer model based on *Rb* cannot be reliably applied to the inhomogeneous estuarine environment where horizontal gradient and advection are important. On the other hand, gradient Richardson number *Ri* based on local shear and density gradient remains a good diagnostic of turbulent mixing in the stratified shear flows considered here.

At the lower-Bay location, the surface mixed layer deepened from 4 m to 9 m between 16 and 18 September (Fig. 7d). The southward winds erode surface stratification and preconditioned the water column for the complete mixing which occurred immediately after landfall. The strong northwestward winds caused an intrusion of saline shelf water into the lower Bay, as shown in Figure 7d. Vertical eddy diffusivity shows a similar increase with time as in the mid-Bay station (Fig. 7e). Strong mixing was confined to the surface and bottom boundary layer before landfall. After landfall the mixing extended throughout the water column with the maximum diffusivity occurring at the mid-depth. Again there is good correspondence between regions of low *Ri* and high Kv (Fig. 7f). These diagnostic analyses at the lower and mid-Bay stations reveal two distinct phases in the evolution of water-column density structure during the passage of Hurricane Isabel: a preconditioning phase where the pre-landfall southward winds drove a gradual deepening of the surface mixed layer and a destratification phase where the post-landfall northward winds caused a rapid destruction of stratification.

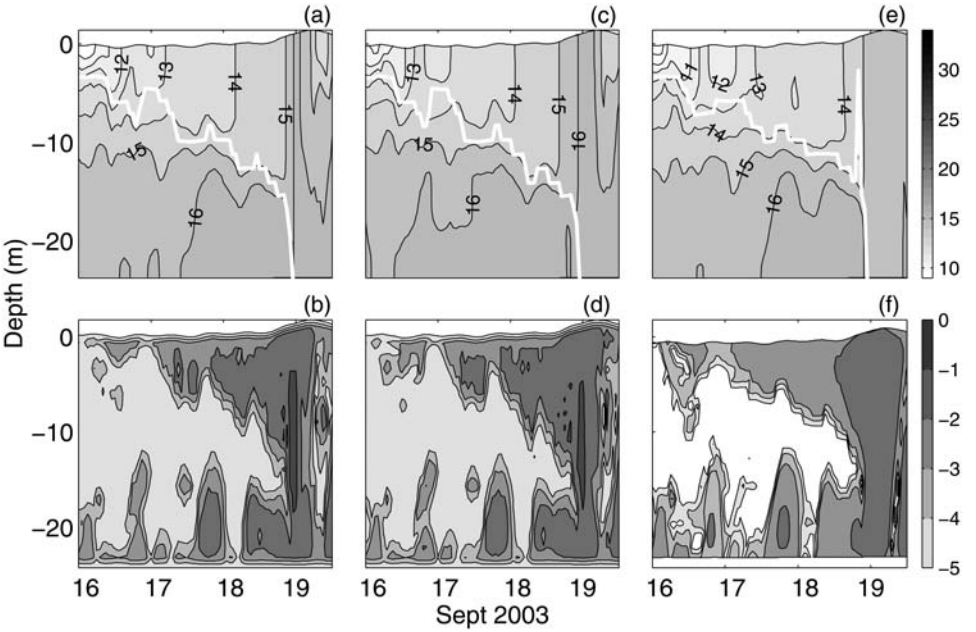

Figure 8. Time evolution of salinity (a, c, e, upper panel) and logarithm of vertical diffusivity ($m^2 s^{-1}$, b, d, f, lower panel) at the mid Bay station obtained from model runs using k-ϵ (a, b), k-ω (c, d) and KPP (e, f) turbulence closure schemes. White lines in the upper panel show the estimated mixed-layer depth.

The *k-kl* (modified Mellor-Yamada) turbulence parameterization scheme incorporated into the ROMS model contains empirical closure assumptions. Are the model results sensitive to the choice of turbulence parameterization? To answer this question, we conducted additional runs using *k*-ϵ, *k*-ω and KPP closure models. Figure 8 compares the predicted salinity and diffusivity distributions between the three schemes. Both k-ϵ and k-ω models give nearly identical results as the *k-kl* model (see Figs. 7a and 7b). The KPP model produces somewhat smaller diffusivities and slower deepening of the surface mixed layer.

The estuary is a highly inhomogeneous environment. Even if salinity is homogenized in the vertical direction, it can still retain large gradients in the horizontal direction. To examine how density structure in the Bay evolves as a whole, we take two snapshots of salinity, vertical diffusivity and *Ri* distributions in the along-channel section: one at 0000 LST 18 September (before landfall) and one at 0000 LST 19 September (after landfall) (Fig. 9). As discussed earlier, the pre-landfall southward winds generated a surface mixed layer. A salinity difference of 3 separated the surface mixed layer from the bottom boundary layer (Fig. 9a). Vertical diffusivity reached 10^{-2} m^2 s^{-1} in the surface mixed layer and 10^{-3} m^2 s^{-3} in the bottom boundary layer (Fig. 9b), while *Ri* fell below ¼ inside these two boundary layers (Fig. 9c). However, the halocline was highly stable with low diffusivity ($Kv < 10^{-4}$ m^2 s^{-1}) and high *Ri* (i.e., $Ri > 1$). After the hurricane made landfall,

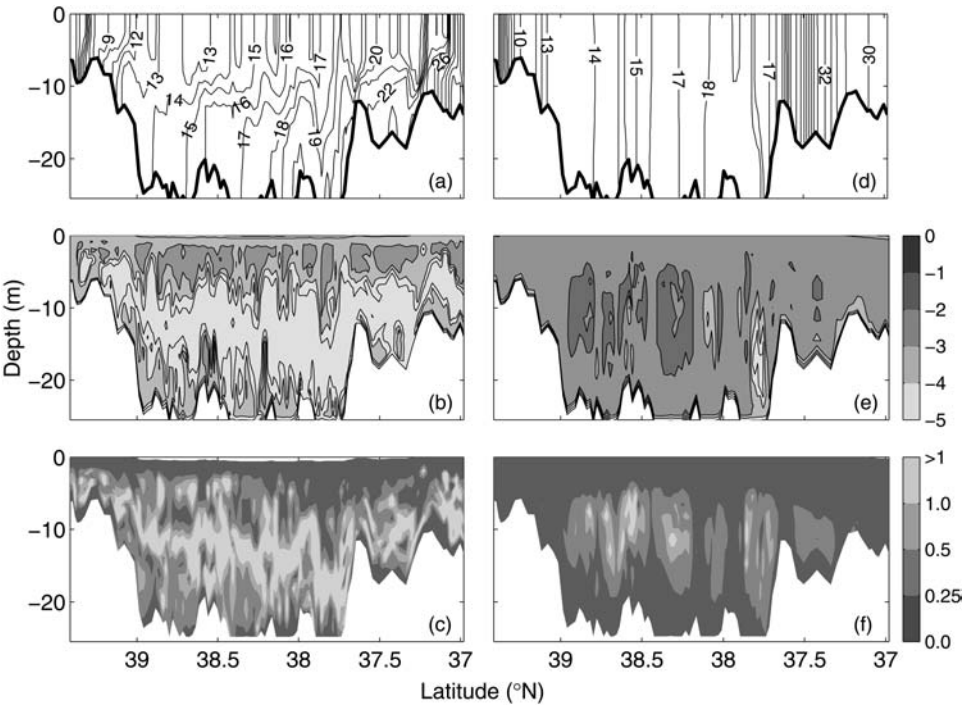

Figure 9. Distribution of (a, d) salinity, (b, e) logarithm of vertical diffusivity and (c, f) gradient Richardson number along the center channel at 0000 LST 18 (left panel) and 0000 LST 19 (right panel) September 2003.

strong northward winds completely erased the stratification, as shown by nearly vertical isohalines in Figure 9d. Hence the hurricane destratified the water column and temporarily transformed the partially-mixed estuary to a vertically homogeneous one. Vertical diffusivity exceeded 10^{-2} m^2 s^{-1} everywhere and reached high values of 0.1 to 1 m^2 s^{-1} at mid-depths (Fig. 9e). Correspondingly, *Ri* fell below ¼ except at mid-depths where ¼<Ri< ½ (Fig. 9f). At the time of complete destratification, the largest diffusivity is found at mid-depth. This result appears to be surprising at first, given that turbulent mixing originates from the surface and bottom boundary layers prior to landfall. The wind stress reached a high value of 1 Nm^{-2} at the storm's peak intensity (see Fig. 5a). This strong wind stress, together with the increasing sea-level slope, drove strong currents which moved the Bay's water as a slab, while the bed stress rose to a maximum of 1.5 Nm^{-2}. This slab flow is similar to turbulent channel flows in which eddy viscosity reaches the maximum value at the mid-depth (cf. Li *et al.*, 2005a).

4. Restratification driven by horizontal density gradient

Hurricane-forced winds erased vertical stratification in Chesapeake Bay shortly after Isabel's landfall. However, a salinity gradient was maintained between the estuary's head

and mouth: the head-to-mouth salinity difference was about 30 (see Fig. 9d). This large horizontal density gradient will lead to restratification since light water tends to move over heavy water. In this section we examine this restratification process.

Simpson and Linden (1989) studied gravitational adjustment of a fluid containing a horizontal density gradient. For the case of uniform horizontal density gradient, they obtain an analytic solution given by

$$N^2 = \frac{1}{2}(\beta g t)^2 \left(\frac{\partial s}{\partial x}\right)^2, \tag{1}$$

$$Ri = \frac{1}{2}, \tag{2}$$

where N is the buoyancy frequency, β the haline contraction coefficient, t the time and $\partial S/\partial x$ the horizontal salinity gradient. According to this theory, the buoyancy frequency is proportional to the horizontal salinity/density gradient and increases linearly with time while Ri is maintained at ½.

When the Coriolis force becomes important, the fluid undergoes geostrophic adjustment. Tandon and Garrett (1994, 1995) obtained an analytic solution for the mixed-layer restratification under the geostrophic adjustment

$$N^2 = (\beta g)^2 \frac{(\partial s/\partial x)^2}{f^2}, \tag{3}$$

$$Ri = 1, \tag{4}$$

where f is the Coriolis parameter. If time-dependence is allowed, inertial oscillations of isopycnals develop and $Ri = ½$.

A comparison of Simpson and Linden's (1989) solution to that of Tandon and Garrett (1994, 1995) suggests that a transition from the gravitational to geostrophic adjustment occurs at a time scale of $\sqrt{2}/f$, i.e., roughly 4 h in the present case. These theoretical calculations assume that no external force is generating turbulent mixing during the adjustment phase while Ri values of ½ or 1 suggest no instability arising from the adjustment itself. We shall test the numerical results against these theoretical predictions.

Isabel's winds reached the peak in the Bay around 0000 LST 19 September and decreased afterwards (Fig. 3b). Although the wind speed decreased gradually during this period, water started to restratify by 1200 LST 19 September. The buildup of stratification was highly non-uniform in space. The buoyancy frequency showed a patchy distribution in the along-channel section (Fig. 10a). The fastest restratification occurred in a near-surface layer (5–10 m depth) where N^2 reached 10^{-3} s^{-2}, as fresher water slid over saline water. Vertical eddy diffusivity reached 10^{-2} m^2 s^{-1} in the lower half of the water column, but was significantly reduced in the upper half, particularly in the near-surface layer where N^2 is highest (Fig. 10b). The water column remained highly unstable to shear instability, as

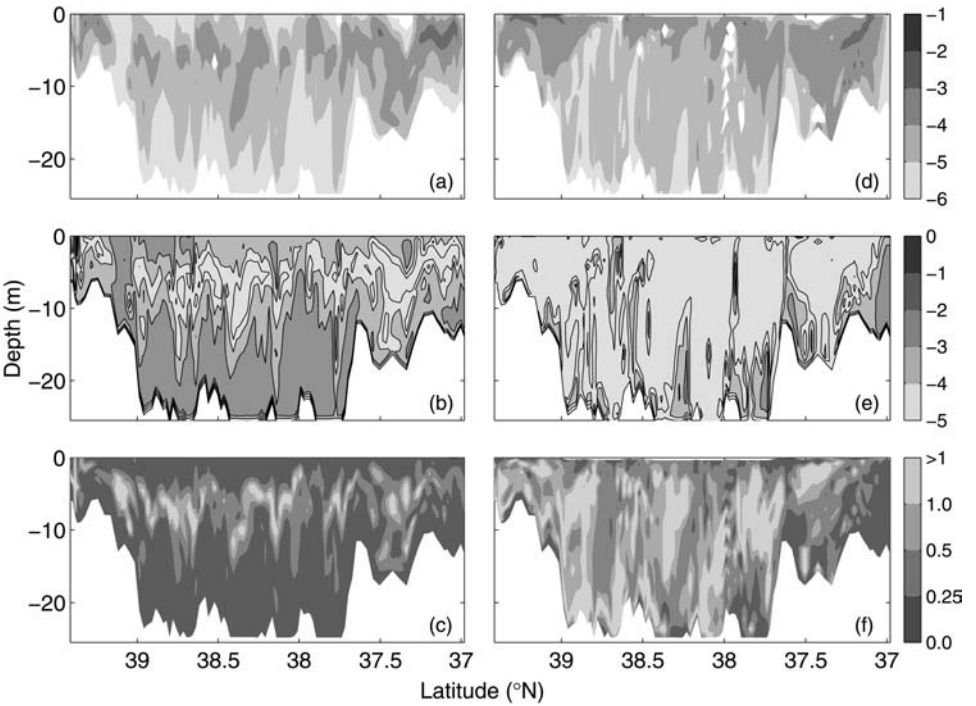

Figure 10. Snapshots of (a, d) logarithm of N^2, (b, e) logarithm of vertical diffusivity and (c, f) gradient Richardson number in the along-channel section at 1200 LST 19 (left panel) and 0000 LST 20 (right panel) September.

indicated by low *Ri* values (Fig. 10c). The enhanced mixing is not caused by the gravitational adjustment but is generated by residual winds and tidal currents acting on weakly stratified water. The wind moderated around 0000 LST 20 September (see Fig. 3b). Stronger stratification developed in the water column by this time, but the buoyancy frequency still displayed patchy distribution (Fig. 10d). The distribution of vertical eddy diffusivity in the along-channel section is given in Figure 10e, which shows that Kv falls below 10^{-4} m^2 s^{-1} in most places in the Bay. This indicates that the strong turbulent mixing appearing earlier weakened markedly by this time. The area where $Ri < 1/4$ shrank to thin bottom boundary layers and the tidally-energetic lower Bay (see Figure 10f, and Zhong and Li, 2006). The region where $Ri > 1/4$ occupied most of the along-channel section, indicating stable water columns with respect to shear instability. This result is qualitatively consistent with that of no shear instability ($Ri = 1/2$) predicted by the gravitational adjustment theory.

Given the horizontal density gradient, both the gravitational and geostrophic adjustment theories provide predictions for the growth of stratification in the water column. In Figure 11 we compare these theoretical predictions against the numerical results. At the time of

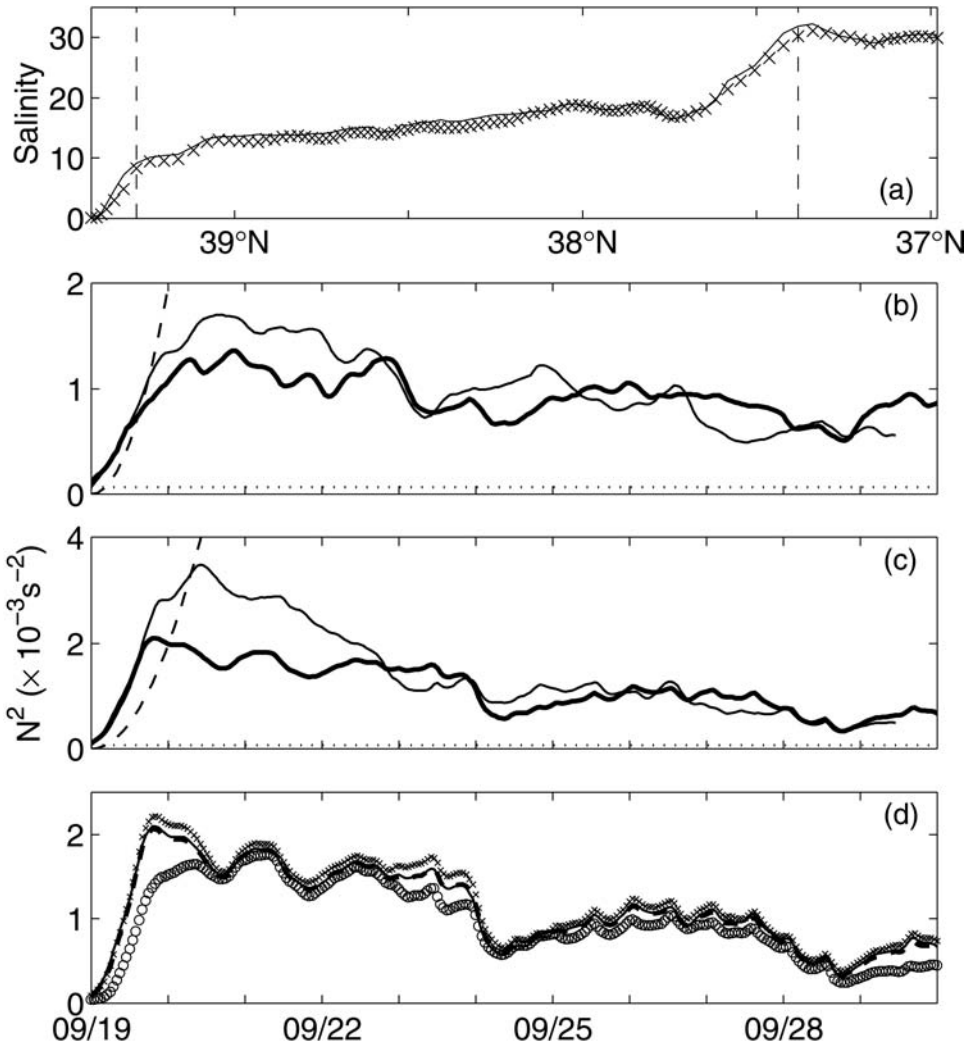

Figure 11. (a) Longitudinal distribution of salinity along the center axis (solid line) and cross-sectional average salinity (cross symbols) at the time of complete destratification. The two vertical dotted lines denote the limits within which N^2 are calculated. Time series of the (b) area- and (c) volume-averaged N^2 obtained from the model runs with the Coriolis force (thick solid) and without the Coriolis force (thin-solid). Dashed (dotted) lines indicate the prediction from the gravitational- (geostrophic-) adjustment theory. (d) Volume-averaged N^2 obtained from the model runs using *k-kl* (solid), *k*-ϵ (dashed), *k*-ω (cross) and KPP (open circles) turbulence closure schemes.

complete mixing, the longitudinal salinity distribution shows nearly uniform gradient except near the estuary's head and mouth. We define the south and north limits within which the buoyancy frequency is calculated. Thus shallow regions in the lower and upper Bay are excluded in the following calculations (see Fig. 9d). We obtain an averaged

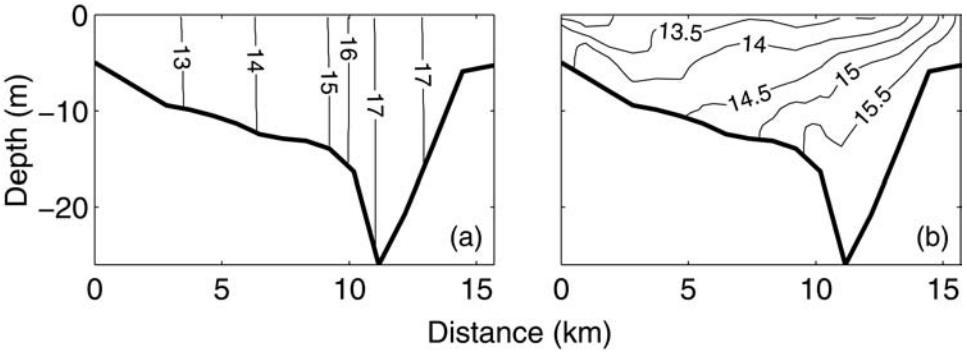

Figure 12. Salinity distribution at a mid-Bay cross section at (a) 0000 LST 19 and (b) 0000 LST 21 September.

horizontal salinity gradient of 9.3×10^{-5} psu m^{-1}. Cross-sectionally averaged salinity shows a similar longitudinal distribution, as shown in Figure 11a. Using the salinity fields obtained from the numerical model, we calculate the averaged stratification (i.e., N^2) in the along-channel section (Fig. 11b). The area-averaged N increased linearly with time and reached about 0.03 s^{-1} 1 day after the destratification. This result is in reasonable agreement with the prediction from the gravitational adjustment theory for the initial period, but exceeds the prediction from the geostrophic adjustment theory. After 24 September, the averaged stratification in the Bay approached a quasi-steady value.

Unlike the open ocean, Chesapeake Bay is a long and relatively-narrow estuary constrained by bathymetry and coastlines. In particular, the presence of sidewall boundaries hinders the development of geostrophic flows in the cross-channel direction. To examine the role of the Earth's rotation in the adjustment process, we conducted another model run in which the Coriolis force is switched off. As shown in Figure 11b, the two model runs with and without the Coriolis force produce similar stratification increases with time, although the nonrotating run gives slightly higher N^2 between 20 and 23 September. This comparison suggests that the Coriolis force plays a secondary role in the restratification process. It thus comes as no surprise that the model results depart from the geostrophic theory.

Although we have so far focused on the restratification in the along-channel section, one should note that the gravitational adjustment is a three-dimensional process. As shown in Li *et al.* (2005b), there are salinity gradients in the cross-channel direction. Figure 12 shows the temporal evolution of salinity distribution in a mid-Bay section. At the peak of the storm, salinity is homogenized vertically but it is higher on the eastern shore than on the western shore by about 4 units (Fig. 12a). Two days later (i.e., 0000 LST 20 September), isohalines are tilted downward towards the western shore, presumably as low-salinity water there spreads over higher-salinity on the eastern shore (Fig. 12b). The Coriolis force likely confines the lower salinity water to the western shore, as demonstrated in Li *et al.* (2005b). The lateral adjustment may affect the gravitational adjustment and restratification in the longitudinal direction. However, the salinity range in any cross-section is much smaller than the salinity difference

between the estuary's head and mouth. The effects of lateral adjustment and restratification are thus expected to be local. A comparison of the volume-averaged N^2 in the Bay to the area-averaged N^2 in the along-channel section shows that the area-averaged and volume-averaged stratification agree within 50% and converge at later times (cf. Figs. 11b and 11c), confirming that the lateral adjustment only plays a secondary role in the longitidudinal restratification process. The difference in the volume-averaged N^2 is again small between the rotating and non-rotating cases. Figure 11d compares the predictions of the volume-averaged N^2 among four model runs using *k-kl*, *k*-ϵ, *k*-ω and KPP turbulence closure schemes. It reveals little differences, suggesting that the predicted post-storm stratification increase is not sensitive to the choice of turbulence mixing parameterization.

After the initial adjustment period of 5 days, salinity distribution in the Bay approached a quasi-equilibrium state, as shown in Figure 13a. Isohalines slope upward toward the sea, as expected in this partially-mixed estuary. However, the top-bottom salinity differences are 2 to 3, which are significantly smaller than those prior to the storm. Therefore, Hurricane Isabel significantly reduced the water-column stratification in the Bay. The tidally-averaged residual velocity shows a two-layer estuarine circulation: seaward in the surface layer and landward in the bottom layer (Fig. 13b). Figure 13c shows the vertical eddy diffusivity in the along-channel section. Due to tidal currents and new wind events, enhanced mixing occurred in the surface and bottom boundary layers as well as in the shallow lower Bay. Hence, turbulent diffusion works against the longitudinal advection to produce a quasi-steady stratification after the passage of Hurricane Isabel.

5. Conclusion

Using a regional atmosphere-ocean model, we have addressed the baroclinic response of Chesapeake Bay to the passage of Hurricane Isabel (2003). Strong hurricane-forced winds caused intense turbulent mixing and complete destratification in the water column, temporarily transforming a partially-mixed estuary into a vertically-homogeneous estuary. After the passage of the storm, the large density gradient between the estuary's head and mouth drove rapid restratification and return to a two-layer estuarine circulation. The coupled destratification and restratification cycle has important implications for the marine ecosystem and water quality. A large phytoplankton bloom was observed in the Bay after Hurricane Isabel (Miller *et al.*, 2006). While mixing and destratification injected benthic nutrients upwards, the subsequent rapid restratification maintained phytoplankton in the well-illuminated surface layer, creating favorable conditions for phytoplankton growth. Mixing and destratification also helped aerate the low-oxygen deep water, but the restratification caused a rapid return of hypoxia to the Bay (Boicourt, 2005). Although Hurricane Isabel did not terminate hypoxia, it significantly reduced the water-column stratification and the impedance to oxygen diffusion across the halocline.

The model results have illustrated the intricate dynamics of storm-driven currents and mixing in a semi-enclosed Bay such as Chesapeake Bay. Prior to the hurricane's landfall, the sea-level slope generated by the local and remote winds worked against the local wind stress in driving the currents. While the southward winds caused the mixed-layer to deepen

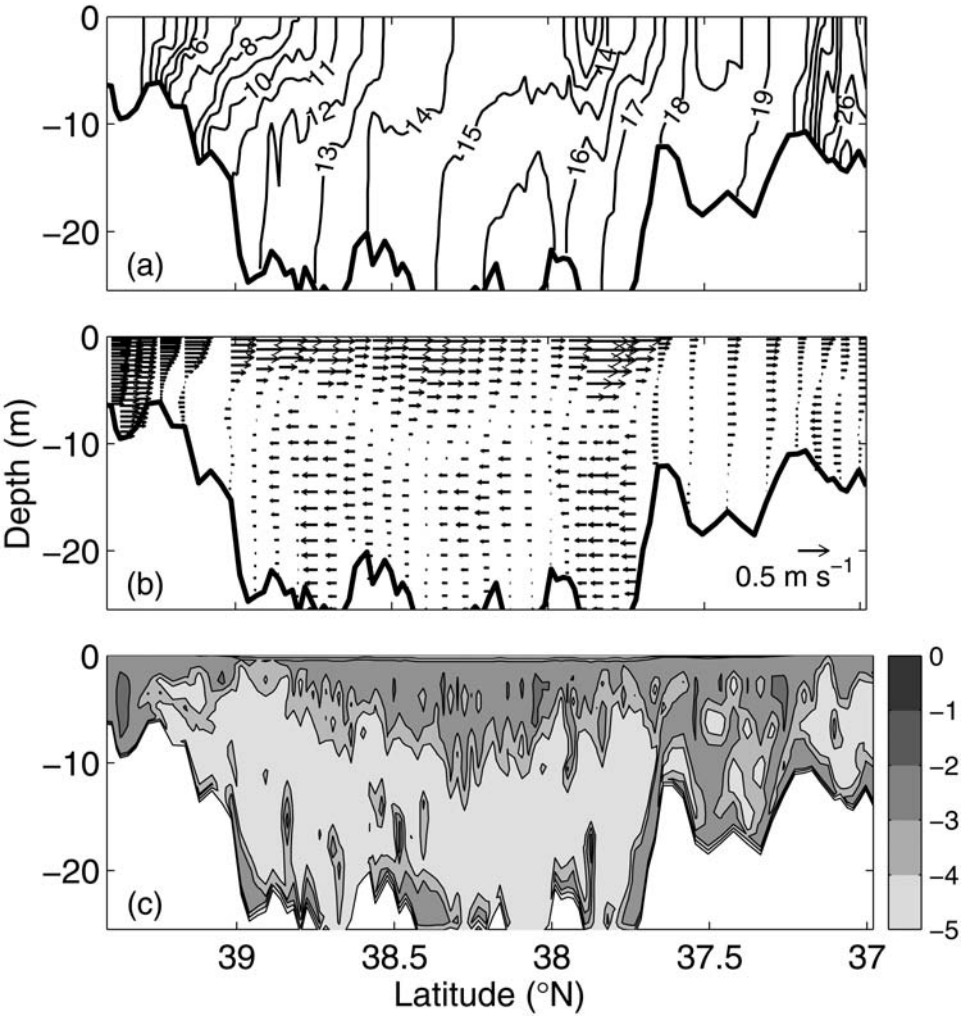

Figure 13. Along-channel distribution of (a) salinity, (b) tidally-averaged residual velocity and (c) logarithm of vertical diffusivity at 0000 LST 30 September 2003.

gradually before landfall, the northward winds caused rapid destratification after landfall. The mixing process does not fit into one-dimensional mixed-layer models but can be interpreted well by the gradient Richardson number and local shear instability. Previous investigations by Goodrich *et al.* (1987) and Blumberg and Goodrich (1990) showed a two-layer response to the local winds and suggested that destratification was driven primarily by the internal shear. Our model simulations of Hurricane Isabel showed a different response due to the combined remote and local wind forcing.

We have also investigated the post-storm restratification and adjustment process driven by the horizontal density gradient. It took about 1 day for significant stratification to return

to the estuary. The averaged buoyancy frequency in the Bay increased linearly with time and reached 0.03 s^{-1} one day after the destratification. This result compares well with the prediction based on the gravitational theory of Simpson and Linden (1989). Subsequently, turbulent mixing due to tides or subsequent winds worked against the gravitational adjustment, putting a brake on the stratification increase and resulting in a quasi-steady salinity distribution in the estuary.

Acknowledgments. This work is supported by grants from NOAA, CICEET, ONR and NSF. We thank Rocky Geyer and Amit Tandon for helpful discussions and two reviewers for their thoughtful comments. This is UMCES contribution number 4056.

REFERENCES

Blumberg, A. F. and D. M. Goodrich. 1990. Modeling of wind-induced destratification in Chesapeake Bay. Estuaries, *13*, 236–249.

Boccaletti, G., R. Ferrari and B. Fox-Kemper. 2007. Mixed-layer instabilities and restratification. J. Phys. Oceanogr., (submitted).

Boicourt, W. C. 2005. Physical response of Chesapeake Bay to hurricanes moving to the wrong side: Refining the forecasts, *in* Hurricane Isabel in Perspective, K. G. Sellner, ed., CRC Press, *5*, 39 – 48.

——1992. The influences of circulation processes on dissolved oxygen in Chesapeake Bay, *in* Dissolved Oxygen in Chesapeake Bay, D. Smith, M. Leffler and G. Mackiernan, eds., Maryland Sea Grant, 7–59.

Brainerd, K. and M. Gregg. 1993a. Diurnal restratification and turbulence in the oceanic surface mixed layer. Part I: Observations. J. Geophys. Res., *98*, 22,645–22,656.

——1993b. Diurnal restratification and turbulence in the oceanic surface mixed layer. Part II: Modeling. J. Geophys. Res., *98*, 22,657–22,664.

Carter, H. H. and D. W. Pritchard. 1988. Oceanography of Chesapeake Bay, *in* Hydrodynamics of Estuaries: Dynamics of Partially-Mixed Estuaries, B. Kjerfve, ed., CRC Press, *1*, 1–16.

Csanady, G.T. 1973. Wind-induced barotropic motions in long lakes. J. Phys. Oceanogr., *2*, 3–13.

Dudhia, J. 1989. Numerical study of convection observed during the winter monsoon experiments using a mesoscale two-dimensional model. J. Atmos. Sci., *46*, 3077–3107.

Egbert, G. D. and S. Y. Erofeeva. 2002. Efficient inverse modeling of barotropic ocean tides. J. Atmos. Ocean. Tech., *19*, 183–204.

Garvine, R. W. 1985. A simple model of estuarine subtidal fluctuations forced by local and remote wind stress. J. Geophys. Res., *90*, 11,945–11,948.

Goodrich, D. M., W. C. Boicourt, P. Hamilton and D. W. Pritchard. 1987. Wind-induced destratification in Chesapeake Bay. J. Phys. Oceanogr., *17*, 2232–2240.

Grell, G. A., J. Dudhia and D. R. Stauffer. 1995. A description of the fifth-generation Penn State/NCAR Mesoscale Model (MM5). NCAR Tech. Note NCAR/TN-398 1 STR, 122 pp.

Janzen, C.D. and K.-C. Wong. 2002. Wind-forced dynamics at the estuary-shelf interface of a large coastal plain estuary. J. Geophys. Res., *107 (C10)*, 3138, doi:10.1029/2001JC000959.

Kain, J. S. and J. M. Fritsch. 1993. Convective parameterization for mesoscale models: The Kain-Fritsch scheme. Cumulus Parameterization. Meteor. Monogr., *46*, 165–170.

Kemp, W. M, W. R. Boynton, J. E. Adolf, D. F. Boesch, W. C. Boicourt, G. Brush, J. C. Cornwell, T. R. Fisher, P. M. Glibert, L. W. Harding, Jr., E. D. Houde, D. G. Kimmel, W. D. Miller, R. I. E. Newell, M. R. Roman, E. M. Smith and J. C. Stevenson. 2005. Eutrophication of Chesapeake Bay: Historical trends and ecological interactions. Mar. Ecol. Progr. Ser., *303*, 1–29.

Li, M and C. Garrett. 1997. Mixed-layer deepening due to Langmuir turbulence. J. Phys. Oceanogr., *27*, 121–132.

Li, M., L. Sanford and S-Y Chao. 2005a. Time-dependent effects in unstratified tidal flows: results from Large Eddy Simulations. Est. Coast. Shelf Sci., *62*, 193–204.

Li, M., L. Zhong and W. C. Boicourt. 2005b. Simulations of Chesapeake Bay estuary: sensitivity to turbulence mixing parameterizations and comparison with observations. J. Geophys. Res., *110*, C12004. doi:10.1029/2004JC002585.

Li, M., L. Zhong, W. C. Boicourt, S. Zhang and D.-L. Zhang. 2006. Hurricane-induced storm surges, currents and destratification in a semi-enclosed bay. Geophys. Res. Lett., *33*, L02604, doi:10.1029/2005GL024992.

Marchesiello, P., J. C. McWilliams and A. F. Shchepetkin. 2001. Open boundary conditions for long-term integration of regional ocean models. Ocean Model., *3*, 1–20.

Miller, W.D., L. W. Harding, Jr. and J. E. Adolf. 2006. The effects of Hurricane Isabel on Chesapeake Bay phytoplankton dynamics. Geophys. Res. Lett., *33*, L06612, doi: 10.1029/2005GL025658.

Roman, M. R., J. E. Adolf, J. Bichy, W. C. Boicourt, L. W. Harding, Jr., E. D. Houde, S. Jung, D. G. Kimmel, W. D. Miller and X. Zhang. 2005. Chesapeake Bay plankton and fish abundance enhanced by Hurricane Isabel. *EOS* Transactions, Amer. Geophys. Union, *86*, 261–265.

Rudnick, D. and R. Ferrari. 1999. Compensation of horizontal temperature and salinity gradients in the ocean mixed layer. Science, *283*, 526–529.

Shchepetkin, A. F. and J. C. McWilliams. 2005. The Regional Oceanic Modeling System: A split-explicit, free-surface, topography-following-coordinate ocean model. Ocean Model., *9*, 347–404.

Simpson, J. E. and P. F. Linden. 1989. Frontogenesis in a fluid with horizontal density gradients. J. Fluid Mech., *202,* 1–16.

Tandon, A.and C. Garrett. 1995. Geostrophic adjustment and restratification of a mixed layer with horizontal density gradients above a stratified layer. J. Phys. Oceanogr., *25*, 2229–2241.

——1994. Mixed layer restratification due to a horizontal density gradient. J. Phys. Oceanogr., *24*, 1419–1424.

Trowbridge, J. H. 1992. A simple description of the deepening and structure of a stably stratified flow driven by a surface stress. J. Geophys. Res., *97*, 15,529–15,543.

Vieira, M. E. C. 1986. The meteorologically driven circulation in mid-Chesapeake Bay. J. Mar. Res., *44*, 473–493.

Wang, D.-P. 1979a. Subtidal sea level variations in the Chesapeake Bay and relation to atmospheric forcing. J. Phys. Oceanogr., *9*, 413–421.

——1979b. Wind-driven circulation in the Chesapeake Bay, winter 1975. J. Phys. Oceanogr., *9*, 564–572.

Warner, J. C., C. R. Sherwood, H. G. Arango, B. Butman and R. P. Signell. 2005. Performance of four turbulence closure models implemented using a generic length scale method. Ocean Model., *8*, 81–113.

Wong, K.-C. and R.W. Garvine. 1984. Observations of wind-induced, subtidal variability in the Delaware estuary. J. Geophys. Res., *89 (C6)*, 10,589–10,597.

Young, W. R. 1994. The subinertial mixed layer approximation. J. Phys. Oceanogr., *24*, 1812–1826.

Zhang, D.-L. 1989. The effect of parameterized ice microphysics on the simulation of vortex circulation with a mesoscale hydrostatic model. Tellus, *41A*, 132–147.

Zhang, D., and R. A. Anthes. 1982. A high-resolution model of the planetary boundary layer—Sensitivity tests and comparisons with SESAME-79 data. J. Appl. Meteor., *21*, 1594–1609.

Zhong, L. and M. Li. 2006. Tidal energy fluxes and dissipation in the Chesapeake Bay. Cont. Shelf Res., *26*, 752–770.

Received: *25 August, 2006* ; revised: *27 February, 2007*.